Accepted Manuscript

Title: Anion–π interactions in active centers of superoxide dismutases

Authors: Vesna R. Ribić, Srđan Đ. Stojanović, Mario V. Zlatović

Please cite this article as: Vesna R.Ribić, Srđan Đ.Stojanović, Mario V.Zlatović, Anion–π interactions in active centers of superoxide dismutases, International Journal of Biological Macromoleculeshttp://dx.doi.org/10.1016/j.ijbiomac.2017.08.050

Anion−π interactions in active centers of superoxide dismutases

Vesna R. Ribić[a], **Srđan Đ. Stojanović[b]**, **Mario V. Zlatović[c,*]**

* Corresponding author.
E-mail address: mario@chem.bg.ac.rs

[a] Institute for Multidisciplinary Research, Department of Materials Science, University of Belgrade, Belgrade, Serbia

[b] ICTM - Department of Chemistry, University of Belgrade, Belgrade, Serbia

[c] Center for Computational Chemistry and Bioinformatics, Faculty of Chemistry, University of Belgrade, Belgrade, Serbia

Abstract

We investigated 1060 possible anion−π interactions in a data set of 41 superoxide dismutase active centers. Our observations indicate that majority of the aromatic residues are capable to form anion−π interactions, mainly by long-range contacts, and that there is preference of Trp over other aromatic residues in these interactions. Furthermore, 68% of total predicted interactions in the dataset are multiple anion−π interactions. Anion−π interactions are distance and orientation dependent. We analyzed the energy contribution resulting from anion−π interactions using *ab initio* calculations. The results showed that, while most of their interaction energies lay in the range from −0 to −4 kcal mol^{-1}, those energies can be up to −9 kcal mol^{-1} and about 34% of interactions were found to be repulsive. Majority of the suggested anion−π interacting residues in ternary complexes are metal-assisted. Stabilization centers for these proteins showed that all the six residues found in predicted anion−π interactions are important in locating one or more of such centers. The anion−π interacting residues in these proteins were found to be highly conserved. We hope that these studies might contribute useful information regarding structural stability and its interaction in future designs of novel metalloproteins.

Keywords

Anion−π interactions · Superoxide dismutase · Proteins · Active centers · Interaction energy

1. Introduction

Due to their crucial roles in stabilising biomolecular structures and in supramolecular chemistry [1–3], noncovalent interactions related to the π electron cloud have gained considerable interest among theoreticians and experimentalists. Among all noncovalent interactions related to aromatic rings, anion–π interactions received the most attention in the last few years. Due to their significant role in aforementioned supramolecular chemistry [4–7], crystal engineering [8–11] and structural biology [12–15], these interactions became a subject of great interest. Anion–π, also referred to as anion-quadrupole, interactions are theorized to form between aromatic groups and anions. Aromatic functional groups are planar and ringed structures with delocalized π electrons. The delocalization of electrons in an aromatic molecule create an electron density above and below the plane of the ring which can be described as a quadrupole (i.e., two opposite dipoles). The direction of the quadrupole creates a positive potential along the plane of an aromatic ring and this allows for favorable interactions with nearly co-planar anions. The general postulation is that electrostatic (charge-quadrupole) and ion-induced polarization (charge-induced dipole) are key forces that contribute to the anion–π interaction [16].

Whereas anion–π interactions were widely studied in supramolecular assemblies, investigation of their role in biological macromolecules is still at its early stages. A systematic search through structures in the Protein Data Bank (PDB) showed that in protein structures orientations similar to those in anion–π interacting pairs exist between standard aromatic residues (Trp, Phe, Tyr, His) and some anions, such as chloride and phosphate [8]. Hinde and co-workers [17] performed a PDB search focusing on interactions between Phe and negatively charged residues, such as Asp and Glu. The interactions having the angle between the anion group and the plane of the ring in the range between 0 to 40º (*edgewise*) were found to be quite common and attractive by their nature (estimated energies were in the range between −8 and −2 kcal mol^{-1}), but the anion–π interactions involving the ring face were less frequent and usually found to be weakly attractive or even slightly repulsive by their nature. Those repulsive forces are usually compensated with other, stronger interaction (salt bridge, H-bonding, or similar; see chapter 3.2). Using the systematic search of protein structures followed by *ab initio*

2

calculations, Deyà and co-workers showed that anion–π interactions are to be expected in flavin-dependent enzymes [18]. Anion–π interactions have been shown to stabilize flavoproteins and to regulate the redox potential of the flavin cofactor [15]. In addition, Moore and co-workers examined high-resolution structures of proteins and nucleic acids for the presence of "η^6"-type anion–π contacts, where the anion is placed directly above the centre of the six-membered ring [12]. Anion–π interactions are currently helpfully exploited in fields such as anion sensing [19–21], supramolecular assembly [7,22,23], and anion transport through membranes [24,25], even in biological systems [18]. Research of the anion channels are of great interest in investigation of diseases such as cystic fibrosis and other anion channelopathies [26]. Sacchettini and co-workers published an outstanding study of the development of effective anti-tuberculosis drugs, reporting an important role of the anion–π interactions [27]. Frontera and co-workers studied long-range effects in anion–π interactions and their role in the mycobacterium tuberculosis malate synthase inhibition mechanism [28], that can be exploited for the development of antitubercular therapeutics because of its significance in *Mycobacterium tuberculosis* virulence. Recently, Matile and co-workers introduce artificial enzymes operating with anion–π interactions [29]. Etezad and co-workers revealed the impact of anion–π interactions in the thermal stability and ionic liquids tolerance that could be used as an alternative strategy to stabilize enzymes using protein engineering [30]. In our recently published works, we suggested that anion–π interactions can contribute significantly to stabilization of Sm/LSm proteins [31], protein-porphyrin complexes [32] and complexes of proteins and halogen-containing amino acids [33].

Superoxide dismutases, or SODs, are enzymes that play a pivotal role in metabolizing $O_2^{\bullet-}$, preempting oxidizing chain reactions that cause extensive damage, and forestalling formation of a cascade of deleterious reactive oxygen species (ROS) including hydrogen peroxide (H_2O_2), hypochlorite (OCl^-), peroxynitrite (ONO_2^-) and hydroxyl radical ($HO^{\bullet}$). The name SOD denotes not one, but three unrelated enzymes. All three earned the name by virtue of ability to convert two molecules of superoxide to one each of dioxygen and hydrogen peroxide, with consumption of two equivalents of H^+. Three classes of SOD have evolved with distinct protein folds and different catalytic metal ions: the Cu/ZnSODs, MnSOD/FeSODs and NiSODs. Cu/ZnSOD (also known as

3

SOD1 and SOD3 in humans) occurs in eukaryotes and some prokaryotes, and point mutations in human Cu/ZnSOD are linked to the fatal neurodegenerative disease amyotrophic lateral sclerosis (ALS, also known as Lou Gehrig's disease). FeSOD and MnSOD (also referred to as SOD2 in humans) appear to have evolved from a common ancestral gene, with the FeSOD gene observed in primitive eukaryotes, the plastids of plants and in bacteria [34–36].

Studies of the metal center in metalloproteins and model systems have shown that many factors, including noncovalent interactions, may play important roles in the properties of these proteins [37–40]. Even though many studies are done on the molecular aspects [34,36], there are no reports on the systematic analysis of noncovalent interactions in superoxide dismutases. Thus, considering the above facts, we thought it would be useful to investigate the role of anion–π interactions in these proteins by bioinformatics approaches. As we focused our study on the active centers, the anion–π interactions within protein structures were not considered. We have investigated the structural stability patterns of anion–π interactions in superoxide dismutases related to the other environmental preferences like preference of particular amino acid residue to form anion–π interactions, interaction geometries and energetic contribution, metal-assisted anion–π interactions in ternary complexes, their involvement in stabilizing centers, and conservation score of anion–π interacting residues. The investigation of these important interactions might enhance our insight of protein stabilities, interaction energies and further improve our understanding of metalloprotein structures and their functions.

2. Materials and methods

2.1. Dataset

For this study, we used the Protein Data Bank (PDB) October 21st, 2015 list of 113,130 structures [41]. The selection criteria for superoxide dismutases to be included in the dataset were (1) crystal structures of proteins containing E.C. Number 1.15.1.1 (superoxide dismutase) with metal were accepted; (2) no theoretical model structures and no NMR structures were accepted, these structur qes were not included since it was difficult to define the accuracy of the ensemble of structures in terms of displacement that

4

was directly comparable to the X-ray diffraction studies; (3) only crystal structures with the resolution of 2.0 Å or better and a crystallographic R-factor of 25.0 % or lower were accepted; and (4) only representatives at 70% sequence identity. After assembling the dataset, several structures containing ligands and mutant amino acids were rejected, thus leaving 41 proteins that were actually used as the dataset in our analysis. Hydrogen atoms were added and optimized where needed, using the program REDUCE [42], with default settings. REDUCE is adding hydrogen atoms to protein and/or DNA structures in standardized geometry optimizing them to the orientations of OH, SH, NH_3^+, Met methyls, Asn and Gln sidechain amides, and His rings. Software determines best hydrogen positions by selecting the best overall score from all of the possible combinations taking into the account individual scores assigned for each individual residue and for groups containing movable protons partitioned in closed sets of local interacting networks. The PDB IDs of these structures are as follows: 1ar5, 1cbj, 1d5n, 1hl5, 1ids, 1isa, 1kkc, 1luv, 1my6, 1qnn, 1srd, 1to4, 1unf, 1xre, 1xuq, 1y67, 1yai, 1yso, 2aqn, 2cw2, 2goj, 2rcv, 2w7w, 3ak2, 3ce1, 3dc6, 3evk, 3f7l, 3h1s, 3js4, 3lio, 3lsu, 3mds, 3pu7, 3tqj, 4br6, 4c7u, 4f2n, 4ffk, 4yet, and 5a9g.

2.2. Anion–π interaction analysis

For selecting the protein structures having various types of possible anion–π interactions some specific criteria and geometrical features were used in Discovery Studio Visualizer 4.5 [43]: (1) Anions (the nearest oxygen atom in Asp or Glu carboxylate group) were considered to be atoms having a formal charge of –0.5 or less. This allowed the inclusion of delocalized anionic species such as aspartate and glutamate side-chains. (2) The distance between an anion and the centroid of a π ring (aromatic moiety from His, Phe, Trp and Tyr) should be less than the anion–π *(max dist)* cut-off (7.0 Å, *R* in Fig. 1). (3) The angle between the anion–centroid vector (line connecting the closest carboxylate oxygen atom and the center point of the π ring) and the normal to the ring plane should be less than the anion–π maximum angle (90°, θ in Fig. 1). Compared to the criteria applied in studies of small molecules found in the CSD (Cambridge Structural Database) these criteria were a bit more relaxed. We opted for slightly looser criteria because the structural variations in crystal structures of proteins are generally

5

larger than in crystal structures of small molecules. Earlier publications confirmed anion–π interactions as long-range interactions, showing notable binding forces even at intermolecular distances of 7 Å [17,32,33,44].

2.3. Computation of anion–π interaction energy

In order to apply *ab initio* methods in determining the energies of predicted anion–π pairs on desired level of theory, calculations were performed on structurally reduced model systems. We used acetate (**1**) as mimics for anionic amino acids (Asp, Glu). Phenylalanine was simplified to methylbenzene (**2**), histidine to 5-methyl-1*H*-imidazole (**3**), while tryptophan and tyrosine were reduced to 3-methyl-1*H*-indole (**4**) and 4-methyphenol (**5**), respectively (Fig. 2).

Ab initio calculations were performed using Jaguar from Schrödinger Suite 2016-1 [45], using LMP2 method with triple zeta Dunning's correlation consistent basis set [46] and ++ diffuse functions [47]. All calculations were performed in vacuum. The LMP2 method applied to the study of anion–π interactions, showed to be considerably faster than the MP2 method while the calculated interaction energies and equilibrium distances are almost identical for both methods [48]. Several authors found that LMP2 represents an excellent method for calculations of interaction energies in proteins [14,49].

Geometries of interacting structures were optimized using LMP2/cc-pVTZ(-f)++ level of theory and their single point energies calculated at LMP2/cc-pVTZ++ level. Optimized geometries were placed in space to match corresponding complexes by superimposing heavy atoms onto their respective coordinates from crystal structures and then the energies of dimeric structures produced in that way were calculated.

The anion–π interaction energies in dimers (anion–π pairs) were calculated as the difference between the energy of the complex and the sum of the energies of the monomers in their optimized geometries.

6

2.4. Computation of stabilization centers

Stabilization centers (SC) are defined as the clusters of residues making cooperative, noncovalent long-range interactions [50]. Measured as individual interactions, stabilisation forces resulting from noncovalent long-range interactions are not very strong, but since they are cooperative by their nature, in regions where they act in a group (SC), they could play an important role in maintaining the overall stability of protein structures. In order to analyze SC of interaction-forming residues, we used the SCide program [51]. The criteria SCide uses for determining SC are as follows: (1) Two residues are in contact if there is, at least, one heavy atom–atom distance smaller than the sum of their van der Waals radii plus 1 Å. (2) A contact is recognized as "long-range" interaction if the interacting residues are, at least, ten amino acids apart. (3) Two residues form a stabilization centers if they are in long-range interaction and if it is possible to select one–one residues from both flanking tetrapeptides of these two residues that make, at least, seven contacts between these two triplets [51].

2.5. Computation of conservation of amino acid residues

The conservation of amino acid residues in each protein was computed using the ConSurf server [52]. This server computes the conservation based on the comparison of the sequence of a PDB chain with the proteins deposited in Swiss–Prot [53] and finds the ones that are homologous to the PDB sequence. The number of PSI–BLAST iterations and the E-value cutoff used in all similarity searches were 1 and 0.001, respectively. All the sequences that were evolutionary related to each one of the proteins in the dataset were used in the subsequent multiple alignments. Based on these protein sequence alignments the residues are classified into nine categories from highly variable to highly conserved. Residues with a score of 1 are considered to be highly variable and residues with a score of 9 are considered to be highly conserved.

3. Results and discussion

In this work, we have analyzed the influence of predicted anion–π interactions in 41 superoxide dismutase structures. Our study focused on the active centers, thus the

eventual anion–π interactions within the rest of the protein structures were not considered. The functions of metal complexes are directly linked to the local environment in which they have profound effects on function that range from the modulation of physical properties to the delivery of reactants and removal of products. Hence, the characteristic features of residues involved in predicted anion–π interactions evaluated were their preference to form anion–π interactions, interaction geometries and energetic contribution, metal-assisted anion–π interactions in ternary complexes, their involvement in stabilizing centers, and conservation score of anion–π interacting residues.

3.1. Preference of residues to form anion–π interactions

The preference of amino acid residues to be involved in predicted anion–π interactions was analyzed and the results for superoxide dismutase active centers are presented in Table 1.

The analysis of the amino acid preferences for the superoxide dismutase active centers allowed us to investigate the amino acid composition of the first and the second coordination sphere of these sites. The most common residues in the first coordination sphere of metal-sites is His, followed by the Asp and H_2O. The analysis of the composition of the second coordination sphere brings two general observations. First, there is a clear trend for metal-sites to be enriched in aromatic residues, particularly in Trp and Tyr. Those residues occurs in this region about 3 times more frequently than their average frequencies in proteins. Second, metal-sites tend to be depleted of charged residues, with Asp having frequencies reduced by 56% with respect to their average frequencies (Table 1). A possible functional requirement for aromatic residues in metal-sites may be due to their ability to mediate electron transfer reactions, which makes them most suitable for tunneling electrons to/from redox sites [54,55].

We found out that suggested anion–π interactions are present in all of the superoxide dismutase active centers. There were a total of 1060 interactions found. On average, in every active center analyzed, we found 7.5 predicted anion–π interactions between the amino acid residues. It is noteworthy that Trp, although less frequently found

8

in this database, was involved in more anion–π interactions than the other aromatic residues. From the inspection of the results in Table 1, it can be reasoned that Asp and Glu have the same preference for the aromatic rings for establishing eventual anion–π interactions. From all of the results obtained in these analyses, we concluded that the contribution of amino acids toward a particular anion–π interaction is specific for these proteins. The findings for this type of proteins differ to some extent from previous results for Sm/LSm proteins [31], protein–porphyrin complexes [32] and complexes of proteins and halogen-containing amino acids [33].

In order to better understand their stabilizing role, in this study we extended the analysis of interactions between the first and the second coordination sphere of superoxide dismutases. We found 447 (42.2%) predicted anion–π interactions between Asp and His from first coordination sphere and surrounding aromatic amino acids (an illustrative example is shown in Fig. 3). The most abundant aromatic amino acid involved in such interactions is Trp (52.3%), followed by His (24.8%), Phe (17.2%), and Tyr (5.7%). It has been suggested that the interaction between ligands coordinated to a metal ion and aromatic residues can represent a kind of cation/anion–π interaction [16,56], which may be important for stabilizing the conformation of metal sites, and for the mechanisms of certain enzymatic reactions occurring at the metal center [29,57].

Clusters of predicted anion–π interactions (involving more than one anion–π pair) were found in the protein structures. Many crystal structures of superoxide dismutases demonstrated that an anion is capable of binding with several aromatic residues. For example, in the crystal structure of superoxide dismutase (Fe) (sodB) from *Coxiella burnetii* (PDB ID: 3tqj), there exists a "π–anion–π" interaction structure motif (Fig. 4a). The negative charged residue is sandwiched by two aromatic residues. This binding motif of an anion interacting with two aromatic residues was also reported earlier in protein structures [17,31–33] and obviously could present a significant factor in maintaining structural stability. Fig. 4b shows the presence of several anions surrounding one aromatic group. The analysis shows that about 68% of the total interacting residues in the dataset are involved in the formation of multiple anion–π interactions. This conveys that

9

furcation is an inherent characteristic of macromolecular crystal structures. All of the studies above showed that different types of anion−π interactions existing in superoxide dismutase active centers could significantly influence their structural stability.

3.2. Interaction geometries and energetic contribution of anion−π interactions

The geometries of interacting pairs observed in our work certainly are not always the one that could show the highest calculated anion–π interaction energy, but the ones that provide the maximum stability to the protein structure by optimizing the use of all interactions that can coexist with other amino acid moieties, along with possible anion–π interaction were interested in. Within a large protein structure numerous interaction are possible, and sometimes it is not easy to parse out the role of the anion–π interaction in their energetics by simple calculation. Therefore, the interacting pair residues participating in other noncovalent interactions were not analyzed.

The frequency distribution of the distance and angle parameters of suggested anion−π interacting pairs were analyzed (Fig. 5). The geometrical details were quantified using the parameters (R, θ) described in the section 2. The plot of distance distribution derived from anion–π interacting pairs, between the anion group and aromatic ring of amino acid residues, shows the distance distribution has a maximum at 5.0–5.5 Å. The shortest distance found was 3.49 Å, as shown in Fig. 5a. The anion–π pair angles were distributed between all values (0 to 90º range), with a preference for larger angle values (Fig. 5b). The histogram reveals two well-defined, asymmetrically represented states which can be easily associated with face-to-face (from 0° to 40°) and edge-to-face (from 50° to 90°) interactions (Fig. 5b). However, the histogram shows that the edge-to-face interactions are unevenly distributed along the considered angles. These calculations clearly indicate that an effective anion–π interaction can be realized across a wider area above the π ring. There was no significant statistical difference observed in the distribution of geometrical parameters when single and multiple anion–π interactions were in question. However, distribution of distance and angle parameters suggested that the packing of side-chains is nonrandom. The analysis of the geometrical parameters for this type of protein anion–π interactions yielded results similar to those obtained for

10

Sm/LSm proteins [31], protein–porphyrin complexes [32] and complexes of proteins and halogen-containing amino acids [33].

The energetic contributions of residues involved in predicted anion–π interactions were computed using *ab initio* calculations at LMP2 level. The energy of anion–π interaction depends upon various factors such as the size and electronic structure of the anion, nature of the π-ligand, extent of ligation, the directionality and interplay with other noncovalent interactions [16,58]. The results of calculations of the interaction energies for all possible interacting pairs are presented in Fig. 6. Calculated energies were in the range from −9.27 to +10.15 kcal mol^{-1}, but most of them were in the range from −4 to 0 kcal mol^{-1}, indicating that the anion–π interactions in proteins can be common and non-negligible. Previously published results reported finding in numerous protein structures anion–π interactions between Phe and negatively charged residues such as Asp and Glu with energies less than −8 kcal mol^{-1} [17,32,59]. The overall interaction energies may also be modulated by the environment of the interacting pairs in the protein. About 66% of calculated energies of interacting anion–π pairs were attractive by nature (values were less than 0), indicating a stabilizing contribution to the corresponding protein structures, but 34% of the calculated interaction energies were repulsive (their calculated values were larger than 0). The repulsive nature of those interactions emerges from the unfavorable geometries of anion–π interactions in the crystal structures and usually is counterbalanced by other interactions. Namely, we mentioned earlier that, when examined under isolated conditions, this type of interaction is considered unfavorable, but similar to other potentially unfavorable interactions, their influence can be compensated by other interactions from the rest of the polypeptide chain [32,33].

The highest predicted attractive anion–π energetic contribution (−9.27 kcal mol^{-1}) is with Asp72 and His88 (PDB ID: 1yai) and the lowest (−0.01 kcal mol^{-1}) is with Asp165 and His150 (PDB ID: 3ak2); the interacting residues with the highest and lowest interaction energies are shown in Fig. 7. Such large differences are caused by distribution

11

of charge and distance, as pictures of electrostatic potential mapped on electron density (**ESP**) in dimer systems shows, and by their orientation in protein. The nature of the anion–π interaction has been initially interpreted in terms of an attractive electrostatic ion–quadrupole interaction [59]. In a case of highest predicted anion–π energetic interaction, electrostatic distribution and orientations are favorable (Fig. 7a), showing greater compatibility and thus adding to stabilizing forces, while in case of lowest energetic interaction the orientation of ESP are not so favorable, (Fig 7b). Furthermore, the distance between two interacting residues is larger, thus making the ion-quadrupole interaction weaker. This is in agreement with calculated electrostatic potential surfaces around aromatics which are a qualitative guide to anion–π interactions.

3.3. Metal-assisted anion–π interactions in ternary complexes

Taking advantage of the structural versatility of metal ions and the directionality of metal-ligand interactions, the spontaneous assembly of elegant supramolecular architectures with unusual properties and applications or intriguing host-guest behaviour was described [5]. In this section, a special type of suggested anion–π interaction is considered, in cases where the aromatic system interacts with an anion and a transition metal on opposing sides of the ring. This kind of predicted interaction we call the metal-assisted anion–π interaction. The metal coordination strongly affects the π-binding ability of the aromatic ligands, increasing significantly their π-acidity and, consequently, enhancing the ability of the ring to interact favourably with anions. Here we focus on the bonding relationship between anionic and aromatic amino acids coordinated to transition metals in ternary complexes of superoxide dismutase active centers.

The search for these specific interactions in proteins returned 447 hits out of 1060 anion–π interactions, implying that 42.2% of the interactions are involved in metal-assisted anion–π interactions. The amino acids directly coordinated to metal ion (first coordination sphere) that participate in the interactions are Asp and His. The most abundant aromatic amino acid from second coordination sphere involved in such interactions is Trp (47.6%), followed by Asp (20.4%), Phe (18.7%), His (7.0%) and Tyr (6.3%). Analyzing the incidences of different kind of metal, we found that Fe^{3+} (25.5%)

12

and Mn^{2+} (25.5%) plays a dominant role. They are followed by Cu^{2+} (19.6%), Zn^{2+} (19.6%), Fe^{2+} (5.9%) and Mn^{3+} (3.9%).

An illustrative example of metal-assisted anion–π interaction is shown in Fig. 8. The zinc active site of Cu/Zn superoxide dismutase from *Neisseria meningitidis* (PDB ID: 2aqn) is depicted. The metal ion (Zn^{2+}) is coordinated in a nearly tetrahedral geometry by three histidyl imidazoles (His104, His113, His122) and an aspartyl residue (Asp125). A second-sphere residue, Asp106, links the metal-binding site by forming anion–π interaction with His122.

In an attempt to evaluate the effect of metal coordination to first-sphere residues on the anion–π interactions we have computed the binding energy of the ternary complexes. The metal-assisted anion–π interactions exhibit large binding energies (about 40%) and shorter distances (about 20%) than those in the corresponding binary anion–π complexes due to the strong electrostatic effect caused by the proximity of the metal center. The metal coordination strongly affects the π-acidity of the aromatic ligand, thus increasing the strength of the anion–π interactions. However, the electronic nature of the other ligands coordinated to the metal influences the interaction strength as well [16,60]. This is a rather unexplored topic that deserves additional investigation. In this respect, several theoretical studies have showed that the contribution of the anion–π interaction is usually large and naturally assisted by the increased electron deficiency induced by coordination [61–63].

3.4. Stabilization center residues

Stabilization centers are composed by residues involved in cooperative long-range contacts, which are likely to play an important role in the regulation of flexibility and the stability of protein structures [50]. The residues most frequently forming stabilization centers are commonly located in buried positions of protein and usually have a hydrophobic or aromatic side-chain, although some polar or charged residues are found as well. The performed structural and sequential conservation analysis showed a higher conservation of stabilization centers over protein families [50,64]. Stabilization centers,

13

which in general protect the protein structure against spontaneous degradation due to thermal fluctuation, have also been used in evolution to develop a simple means for regulating the house-keeping of an immunologically important protein family, the classical MHC molecules [65,66].

We have computed the stabilization centers for all predicted anion−π interaction forming residues in superoxide dismutase active centers using the SCide program and the results are depicted in Table 2. It was found that 31.7% of anionic residues and 36.0% of π residues were found to have one or more stabilization centers. Among the stabilization centers involving π residues, His and Phe were incorporated more frequently than other residues. Since considerable number of anion−π interacting residues have more than one stabilization center, these residues confers additional stability to the protein along with their participation in anion−π interactions. It is interesting to note that these results are comparable with findings in anion−π interaction studies in Sm/LSm proteins [31] but different than our results from investigation of anion−π interaction in protein–porphyrin complexes [32] and complexes of proteins and halogen-containing amino acids [33].

3.5. Conservation score of anion−π interacting residues

The level of evolutionary conservation was used often as indicator for the importance of the position in maintaining the protein's structure and/or function [67]. Functionally important residues are identified based on the conservation score generated by ConSurf server. From our analysis, we found that more than 81% of predicted anion−π interacting residues are conserved (the cutoff value used to identify the stabilizing residues was conservation score ≥6). Of all of the interacting residues, 22.3% had the highest conservation score, 9. Moreover, most of the additional residues comprising the superoxide dismutase active centers show a great degree of conservation as well.

Considering metal-assisted residues we found that 51.2% of the residues have the highest conservation score of 9, while 48.8% of the residues are in the range of 6–8. In the case of non-metal-assisted residues we found that 14.3% of residues have the highest

14

conservation score of 9 and 52.0% of the residues are in the range of 6–8. Thus 100% of metal-assisted residues and 66.3% of non-metal-assisted residues have a higher conservation score of 6 and above (Fig. 9). Those results indicate higher level of evolutionary conservation in case of metal-assisted residues than in non-metal assisted residues and can indicate their functional importance in function and structure of protein.

Since the conserved residues plays an important role in the stability and functional specificity of protein structure, results obtained from this study could be useful for understanding the importance of anion–π interacting residues in the stability of superoxide dismutase.

As a representative picture, the conservation grade of amino acid residues in Cu/Zn superoxide dismutase from *Neisseria meningitidis* (PDB ID code 2aqn; Chain A) using Chimera [68] is shown in Fig. 10. Conservation score of anion–π interacting residues (A:Asp106 and A:His122) is 9.

Evolutionary conservation interacting pairs position in proteins was further examined using the multiple structural alignment. The structural similarity of the proteins was carried using PDBeFold server [69]. The PDB coordinates, downloaded from RCSB website, were uploaded to the server for finding structural similarity. PDBeFold structural similarity searches were conducted using on-line interface of web server at http://www.ebi.ac.uk/msd-srv/ssm/. The PDBeFold compares structures by matching the graph built on secondary-structure elements, followed by iterative 3D alignment of protein backbone Cα atoms. Due to their diversification, all superoxide dismutase structures could not be aligned, therefore structures were grouped according to the type of metal ion in protein (FeSOD, MnSOD and Cu/ZnSOD). Alignment scores and positions of matched/unmatched residues of all proteins in group, generated for the multiple structural alignment are shown in Supplementary material. Quite interestingly, almost of all the structures considered in this study retain similar three-dimensional folding, as revealed by the low RMSD values. Analysis of the residue-by-residue 3D-mapping data

(in a similar way it was done by ConSurf alignment) also indicates high degree of similarity observed in metal-assisted anion–π interaction residues (Supplementary material; 3D Structural alignment tab). We observed that 100% of metal-assisted anion–π interaction and 83% of non-metal-assisted anion–π interaction positions were conserved. The present study reveals that, in general, interacting positions have structural convergence with respect to anion–π interactions, which often play important role for maintaining protein function/structure during the evolutionary process.

4. Conclusions

Suggested anion–π interactions are directional non-covalent bonds, distance and orientation dependent. In our investigation, we have studied the role of anion–π interactions in active centers of series of superoxide dismutases and their environmental preferences. We found that most of the aromatic residues located in active centers exhibit anion–π interactions. We investigated the preferences of residues to form predicted anion–π interactions and results we obtained suggest that Trp is most abundant anion–π interacting residue, whereas Phe has the lowest occurrence of anion–π interactions in the dataset we studied. Furthermore, the multiple interaction patterns founded in the present study indicate that more than half of the residues involved in these interactions participate in multiple anion–π interactions. The results of *ab initio* calculations of optimized structures of interacting anion–π pairs showed that approximately 34% of those interactions are repulsive by their nature. The energy favorable interactions were less than –9 kcal mol^{-1}, while most of them have energy in the range from 0 to –4 kcal mol^{-1}. Our analysis found that majority of the anion–π interacting residues in ternary complexes are metal-assisted. moreover, significant percentage of anion–π interacting residues are located in stabilization centers as well, and thus capable to provide additional stability of these proteins. Occurrence of significant percentage of anion–π interacting residues in highly conserved region could indicate the important role these interactions possess in superoxide dismutases. Having all of this in mind, we hope that these studies might contribute useful information regarding structural stability and its interaction in future designs of novel metalloproteins.

Acknowledgements

References

[1] K. Muller-Dethlefs, P. Hobza, Noncovalent interactions: a challenge for experiment and theory, Chem. Rev. 100 (2000) 143-168.

[2] E.A. Meyer, R.K. Castellano, F. Diederich, Interactions with aromatic rings in chemical and biological recognition, Angew. Chem. Int. Ed. Engl. 42 (2003) 1210-1250.

[3] M. Chourasia, G.M. Sastry, G.N. Sastry, Aromatic-Aromatic Interactions Database, A^2ID: an analysis of aromatic π-networks in proteins, Int. J. Biol. Macromol. 48 (2011) 540-552.

[4] G. Aragay, A. Frontera, V. Lloveras, J. Vidal-Gancedo, P. Ballester, Different nature of the interactions between anions and HAT(CN)6: from reversible anion−π complexes to irreversible electron-transfer processes (HAT(CN)6 = 1,4,5,8,9,12-hexaazatriphenylene), J. Am. Chem. Soc. 135 (2013) 2620-2627.

[5] H.T. Chifotides, I.D. Giles, K.R. Dunbar, Supramolecular architectures with π-acidic 3,6-bis(2-pyridyl)-1,2,4,5-tetrazine cavities: role of anion−π interactions in the remarkable stability of Fe(II) metallacycles in solution, J. Am. Chem. Soc. 135 (2013) 3039-3055.

[6] N. Mohan, C.H. Suresh, Anion receptors based on highly fluorinated aromatic scaffolds, J. Phys. Chem. A 118 (2014) 4315-4324.

[7] L.M. Eytel, A.K. Gilbert, P. Gorner, L.N. Zakharov, D.W. Johnson, M.M. Haley, Do CH-anion and anion−π interactions alter the mechanism of 2:1 host-guest complexation in arylethynyl monourea anion receptors?, Chemistry 23 (2017) 4051-4054.

[8] A. Robertazzi, F. Krull, E.W. Knapp, P. Gamez, Recent advances in anion−π interactions, CrystEngComm 13 (2011) 3293-3300.

[9] T.J. Mooibroek, P. Gamez, Directional character of solvent- and anion-pentafluorophenyl supramolecular interactions, CrystEngComm 14 (2012) 3902-3906.

[10] N. Hafezi, J.M. Holcroft, K.J. Hartlieb, E.J. Dale, N.A. Vermeulen, C.L. Stern, A.A. Sarjeant, J.F. Stoddart, Modulating the binding of polycyclic aromatic hydrocarbons inside a hexacationic cage by anion−π interactions, Angew. Chem. 127 (2015) 466-471.

[11] A. Bauzá, T.J. Mooibroek, A. Frontera, Towards design strategies for anion−π interactions in crystal engineering, CrystEngComm 18 (2016) 10-23.

[12] S. Chakravarty, Z.Z. Sheng, B. Iverson, B. Moore, "η^6"-Type anion−π in biomolecular recognition, FEBS Lett. 586 (2012) 4180-4185.

[13] D.D. Jenkins, J.B. Harris, E.E. Howell, R.J. Hinde, J. Baudry, STAAR: statistical analysis of aromatic rings, J. Comput. Chem. 34 (2013) 518-522.

[14] G.J. Jones, A. Robertazzi, J.A. Platts, Efficient and accurate theoretical methods to investigate anion−π interactions in protein model structures, J. Phys. Chem. B 117 (2013) 3315-3322.

[15] Y.P. Yurenko, S. Bazzi, R. Marek, J. Kozelka, Anion−π interactions in flavoproteins involve a substantial charge-transfer component, Chemistry 23 (2017) 3246-3250.

[16] A. Frontera, P. Gamez, M. Mascal, T.J. Mooibroek, J. Reedijk, Putting anion−π interactions into perspective, Angew. Chem. Int. Ed. Engl. 50 (2011) 9564-9583.

[17] V. Philip, J. Harris, R. Adams, D. Nguyen, J. Spiers, J. Baudry, E.E. Howell, R.J. Hinde, A survey of aspartate-phenylalanine and glutamate-phenylalanine interactions in the protein data bank: searching for anion−π pairs, Biochemistry 50 (2011) 2939-2950.

[18] C. Estarellas, A. Frontera, D. Quiňonero, P.M. Deyà, Anion−π interactions in flavoproteins, Chem. Asian J. 6 (2011) 2316-2318.

[19] S. Guha, S. Saha, Fluoride ion sensing by an anion−π interaction, J. Am. Chem. Soc. 132 (2010) 17674-17677.

[20] S. Nadella, P.M. Selvakumar, E. Suresh, P.S. Subramanian, M. Albrecht, M. Giese, R. Fröhlich, Lanthanide(III) complexes of bis-semicarbazone and bis-imine-substituted phenanthroline ligands: solid-state structures, photophysical properties, and anion sensing, Chemistry 18 (2012) 16784-16792.

[21] S. Saha, B. Akhuli, I. Ravikumar, P.S. Lakshminarayanan, P. Ghosh, Recognition of fluoride in fluorophenyl attached tripodal amide receptors: structural evidence of solvent capped encapsulation of anion in a C_{3v}-symmetric tripodal cleft, CrystEngComm 16 (2014) 4796-4804.

[22] A. Vargas Jentzsch, A. Hennig, J. Mareda, S. Matile, Synthetic ion transporters that work with anion−π interactions, halogen nonds, and anion−macrodipole interactions, Acc. Chem. Res. 46 (2013) 2791-2800.

[23] V. Kane Dickson, L. Pedi, S.B. Long, Structure and insights into the function of a Ca^{2+}-activated Cl^- channel, Nature 516 (2014) 213-218.

[24] A. Campo-Cacharrón, E.M. Cabaleiro-Lago, I.n. González-Veloso, J. Rodríguez-Otero, Interaction of anions with substituted buckybowls. The anion`s nature and solvent effects, J. Phys. Chem. A 118 (2014) 6112-6124.

[25] X. Fang, M.D. Guo, L.J. Weng, Y. Chen, M.J. Lin, Cooperative effect of anion−π and electrostatic interactions in NIR absorbing phenolate naphthalene diimide conjugates, Dyes and Pigments 113 (2015) 251-256.

[26] S. Durupt, S. Mazur, P. Reix, La mucoviscidose en 2014: actualités thérapeutiques, Rev. Pneumol. Clin. 72 (2016) 77-86.

[27] I.V. Krieger, J.S. Freundlich, V.B. Gawandi, J.P. Roberts, V.B. Gawandi, Q. Sun, J.L. Owen, M.T. Fraile, S.I. Huss, J.L. Lavandera, T.R. Ioerger, J.C. Sacchettini, Structure-guided discovery of phenyl-diketo acids as potent inhibitors of M. tuberculosis malate synthase, Chem. Biol. 19 (2012) 1556-1567.

[28] A. Bauzá, D. Quiňonero, P.M. Deyà, A. Frontera, Long-range effects in anion−π interactions: their crucial role in the inhibition mechanism of Mycobacterium tuberculosis malate synthase, Chemistry 20 (2014) 6985-6990.

[29] Y. Cotelle, V. Lebrun, N. Sakai, T.R. Ward, S. Matile, Anion−π enzymes, ACS Cent. Sci. 2 (2016) 388-393.

[30] B. Dabirmanesh, K. Khajeh, F. Ghazi, B. Ranjbar, S.M. Etezad, A semi-rational approach to obtain an ionic liquid tolerant bacterial laccase through π-type interactions, Int. J. Biol. Macromol. 79 (2015) 822-829.

[31] L.M. Breberina, M.K. Milčić, M.R. Nikolić, S.Đ. Stojanović, Contribution of anion−π interactions to the stability of Sm/LSm proteins, J Biol Inorg Chem 20 (2015) 475-485.

[32] M.V. Zlatović, S.Z. Borozan, M.R. Nikolić, S. Đ. Stojanović, Anion−π interactions in protein-porphyrin complexes, RSC Adv. 5 (2015) 38361-38372.

[33] S.Z. Borozan, M.V. Zlatović, S.Đ. Stojanović, Anion−π interactions in complexes of proteins and halogen-containing amino acids, J. Biol. Inorg. Chem. 21 (2016) 357-368.

[34] J.J. Perry, D.S. Shin, E.D. Getzoff, J.A. Tainer, The structural biochemistry of the superoxide dismutases, Biochim. Biophys. Acta 1804 (2010) 245-262.

[35] A.F. Miller, Superoxide dismutases: ancient enzymes and new insights, FEBS Lett. 586 (2012) 585-595.

[36] Y. Sheng, I.A. Abreu, D.E. Cabelli, M.J. Maroney, A.F. Miller, M. Teixeira, J.S. Valentine, Superoxide dismutases and superoxide reductases, Chem. Rev. 114 (2014) 3854-3918.

[37] E.N. Salgado, R.J. Radford, F.A. Tezcan, Metal-directed protein self-assembly, Acc. Chem. Res. 43 (2010) 661-672.

[38] R.L. Shook, A.S. Borovik, Role of the secondary coordination sphere in metal-mediated dioxygen activation, Inorg. Chem. 49 (2010) 3646-3660.

[39] T.L. Olson, J.C. Williams, J.P. Allen, Influence of protein interactions on oxidation/reduction midpoint potentials of cofactors in natural and de novo metalloproteins, Biochim. Biophys. Acta 1827 (2013) 914-922.

[40] S.A. Cook, A.S. Borovik, Molecular designs for controlling the local environments around metal ions, Acc. Chem. Res. 48 (2015) 2407-2414.

[41] P.W. Rose, B. Beran, C. Bi, W.F. Bluhm, D. Dimitropoulos, D.S. Goodsell, A. Prlic, M. Quesada, G.B. Quinn, J.D. Westbrook, J. Young, B. Yukich, C. Zardecki, H.M. Berman, P.E. Bourne, The RCSB Protein Data Bank: redesigned web site and web services, Nucleic Acids Res. 39 (2011) D392-D401.

[42] J.M. Word, S.C. Lovell, J.S. Richardson, D.C. Richardson, Asparagine and glutamine: using hydrogen atom contacts in the choice of side-chain amide orientation, J. Mol. Biol. 285 (1999) 1735-1747.

[43] Accelrys Software Inc., (2015) Discovery Studio Visualizer, Release 4.5. Accelrys Software Inc., San Diego.

[44] M.R. Jackson, R. Beahm, S. Duvvuru, C. Narasimhan, J. Wu, H.N. Wang, V.M. Philip, R.J. Hinde, E.E. Howell, A preference for edgewise interactions between aromatic rings and carboxylate anions: the biological relevance of anion-quadrupole interactions, J. Phys. Chem. B 111 (2007) 8242-8249.

[45] Schrödinger Release 2016-1: Jaguar, Schrödinger, LLC, New York, NY, 2016

[46] T.H. Dunning, Gaussian basis sets for use in correlated molecular calculations. I. The atoms boron through neon and hydrogen, J. Chem. Phys. 90 (1989) 1007-1023.

[47] T. Clark, J. Chandrasekhar, G.n.W. Spitznagel, P.V.R. Schleyer, Efficient diffuse function-augmented basis sets for anion calculations. III. The 3-21+G basis set for first-row elements, L–F, J. Comput. Chem. 4 (1983) 294-301.

19

[48] A.D. Bochevarov, E. Harder, T.F. Hughes, J.R. Greenwood, D.A. Braden, D.M. Philipp, D. Rinaldo, M.D. Halls, J. Zhang, R.A. Friesner, Jaguar: A high-performance quantum chemistry software program with strengths in life and materials sciences, Int. J. Quantum Chem. 113 (2013) 2110-2142.

[49] K.E. Riley, J.A. Platts, J. Řezáč, P. Hobza, J.G. Hill, Assessment of the performance of MP2 and MP2 variants for the treatment of noncovalent interactions, J. Phys. Chem. A 116 (2012) 4159-4169.

[50] Z. Dosztányi, A. Fiser, I. Simon, Stabilization centers in proteins: identification, characterization and predictions, J. Mol. Biol. 272 (1997) 597-612.

[51] Z. Dosztányi, C. Magyar, G. Tusnády, I. Simon, SCide: identification of stabilization centers in proteins, Bioinformatics 19 (2003) 899-900.

[52] H. Ashkenazy, E. Erez, E. Martz, T. Pupko, N. Ben-Tal, ConSurf 2010: calculating evolutionary conservation in sequence and structure of proteins and nucleic acids, Nucleic Acids Res. 38 (2010) W529-W533.

[53] B. Boeckmann, A. Bairoch, R. Apweiler, M.C. Blatter, A. Estreicher, E. Gasteiger, M.J. Martin, K. Michoud, C. O'Donovan, I. Phan, S. Pilbout, M. Schneider, The SWISS-PROT protein knowledge base and its supplement TrEMBL in 2003, Nucleic Acids Res. 31 (2003) 365-370.

[54] J.R. Winkler, Electron tunneling pathways in proteins, Curr. Opin. Chem. Biol. 4 (2000) 192-198.

[55] H.B. Gray, J.R. Winkler, Long-range electron transfer, Proc. Natl. Acad. Sci. USA 102 (2005) 3534-3539.

[56] J.C. Ma, D.A. Dougherty, The cation−π interaction, Chem. Rev. 97 (1997) 1303-1324.

[57] S.D. Zarić, D.M. Popović, E.W. Knapp, Metal ligand aromatic cation−π interactions in metalloproteins: ligands coordinated to metal interact with aromatic residues, Chemistry 6 (2000) 3935-3942.

[58] P. Gamez, The anion−π interaction: naissance and establishment of a peculiar supramolecular bond, Inorg. Chem. Front. 1 (2014) 35-43.

[59] K. Kapoor, M.R. Duff, A. Upadhyay, J.C. Bucci, A.M. Saxton, R.J. Hinde, E.E. Howell, J. Baudry, Highly dynamic anion-quadrupole networks in proteins, Biochemistry 55 (2016) 6056-6069.

[60] A. Frontera, Encapsulation of anions: Macrocyclic receptors based on metal coordination and anion−π interactions, Coord. Chem. Rev. 257 (2013) 1716-1727.

[61] C. Biswas, M.G.B. Drew, D. Escudero, A. Frontera, A. Ghosh, Anion−π, lone-pair−π, π−π and hydrogen-bonding interactions in a Cu^{II} complex of 2-picolinate and protonated 4,4`-bipyridine: Crystal structure and theoretical studies, Eur. J. Inorg. Chem. 2009 (2009) 2238-2246.

[62] S. Brooker, N.G. White, A. Bauzá, P.M. Deyá, A. Frontera, Understanding the forces that govern packing: a density functional theory and structural investigation of anion−π−anion and nonclassical C-H··anion interactions, Inorg. Chem. 51 (2012) 10334-10340.

[63] P. Kar, R. Biswas, M.G. Drew, A. Frontera, A. Ghosh, Host-guest supramolecular interactions in the coordination compounds of 4,4'-azobis(pyridine) with MnX_2 (X = NCS^-, $NCNCN^-$, and PF_{6-}): structural analyses and theoretical study, Inorg. Chem. 51 (2012) 1837-1851.

[64] C. Magyar, M.M. Gromiha, G. Pujadas, G.E. Tusnady, I. Simon, SRide: a server for identifying stabilizing residues in proteins, Nucleic Acids Res. 33 (2005) W303-W305.

[65] Á. Simon, Z. Dosztányi, C. Magyar, G. Szirtes, É. Rajnavölgyi, I. Simon, Stabilization centers and protein stability, Theor. Chem. Acc. 106 (2001) 121-127.

[66] M. Bello, J. Correa-Basurto, Molecular dynamics simulations to provide insights into epitopes coupled to the soluble and membrane-bound MHC-II complexes, PLoS One 8 (2013) e72575.

[67] M. Landau, I. Mayrose, Y. Rosenberg, F. Glaser, E. Martz, T. Pupko, N. Ben-Tal, ConSurf 2005: the projection of evolutionary conservation scores of residues on protein structures, Nucleic Acids Res. 33 (2005) W299-W302.

[68] E.F. Pettersen, T.D. Goddard, C.C. Huang, G.S. Couch, D.M. Greenblatt, E.C. Meng, T.E. Ferrin, UCSF Chimera−A visualization system for exploratory research and analysis, J. Comput. Chem. 25 (2004) 1605-1612.

[69] E. Krissinel, K. Henrick, Secondary-structure matching (SSM), a new tool for fast protein structure alignment in three dimensions, Acta Crystallogr. D. Biol. Crystallogr. 60 (2004) 2256-2268.

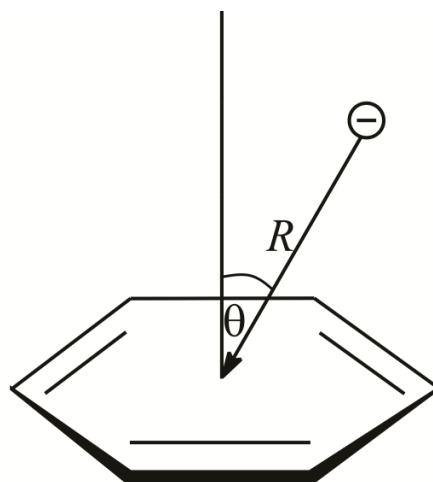**Fig. 1.** Parameters for anion−π interactions: the distance (R) between the anion and the centroid of the ring; and the angle (θ) between the anion−centroid vector and the principle axis of the aromatic ring.
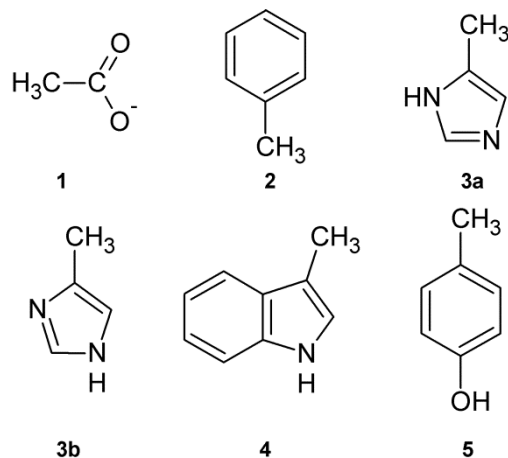
Fig. 2. Structurally reduced structures used for calculations of anion–π interaction energy. (**1**) instead of carboxylate from Asp and/or Glu; (**2**) instead of Phe; (**3a**) or (**3b**) instead of His; (**4**) instead of Trp; (**5**) instead of Tyr.
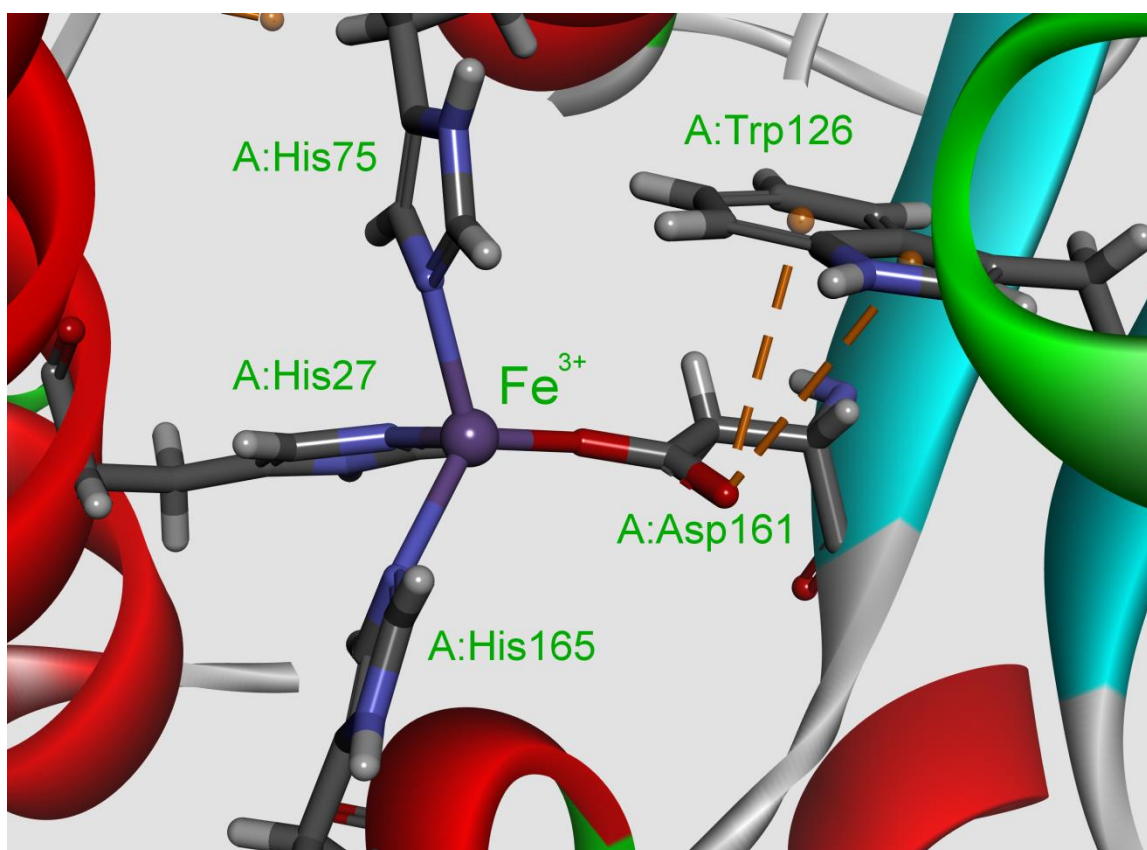

Fig. 3. The predicted anion–π interaction between the first and the second coordination sphere of cambialistic superoxide dismutase from *Propionibacterium shermanii* (PDB ID: 1ar5). The anion–π interaction is marked *with brown dashed lines* (A:Asp161:OD1—

A:Trp126). The indole group of tryptophan consists of two aromatic rings: one five-membered and one six-membered. Both can take part in anion–π interaction and they can even do this simultaneously. Angle θ between anion and ring centroids is 18.75° for six-membered ring and 27.27° for five-membered ring. This particular interaction is calculated as slightly repulsive (E_{int} = +0.7 kcal mol^{-1}). Letters followed by the colon (e.g. A:) in front of the amino acid name on the picture are names of the protein chain. Figure was prepared using the program Discovery Studio Visualizer 4.5 [43].
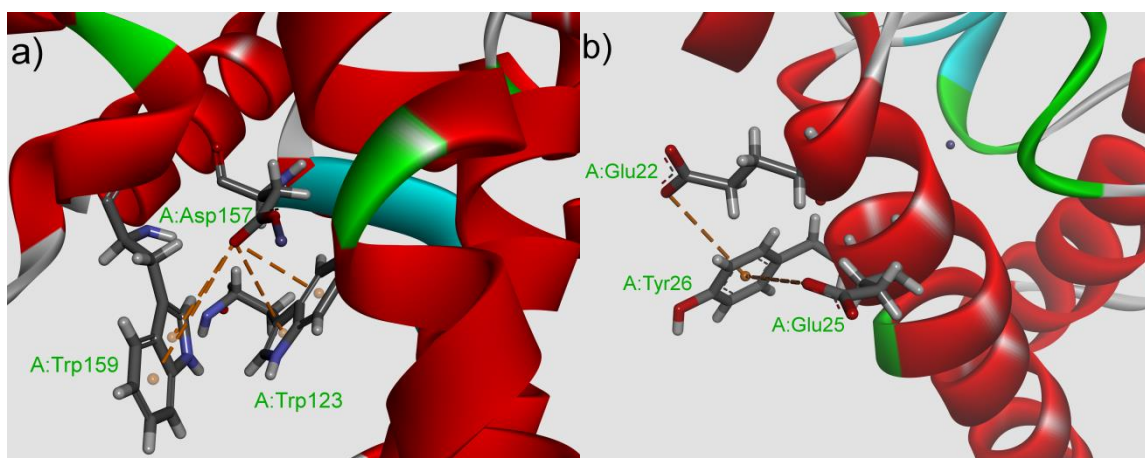

Fig. 4. Details of multiple anion–π interactions of superoxide dismutase (Fe) (sodB) from *Coxiella burnetii* (PDB ID: 3tqj). (a) An anion with multiple aromatics. (b) Several anions clustering around an aromatic group. The anion–π interactions are marked *with brown dashed lines*. Letters followed by the colon (e.g. A:) in front of the amino acid name on the picture are names of the protein chain. Figure was prepared using the program Discovery Studio Visualizer 4.5 [43].
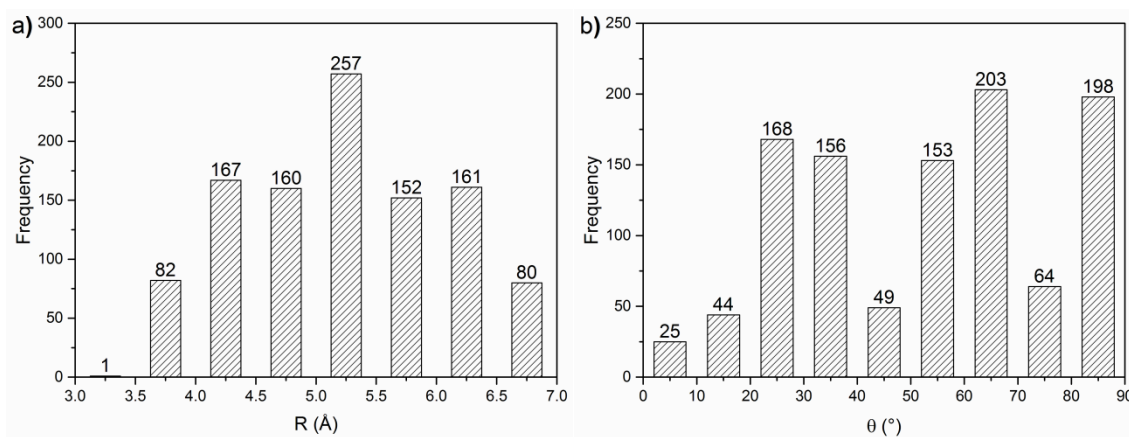
Fig. 5. Distributions of interaction geometries. (a) Distance distribution of anion−π interactions. (b) θ angle distribution of anion−π interactions.
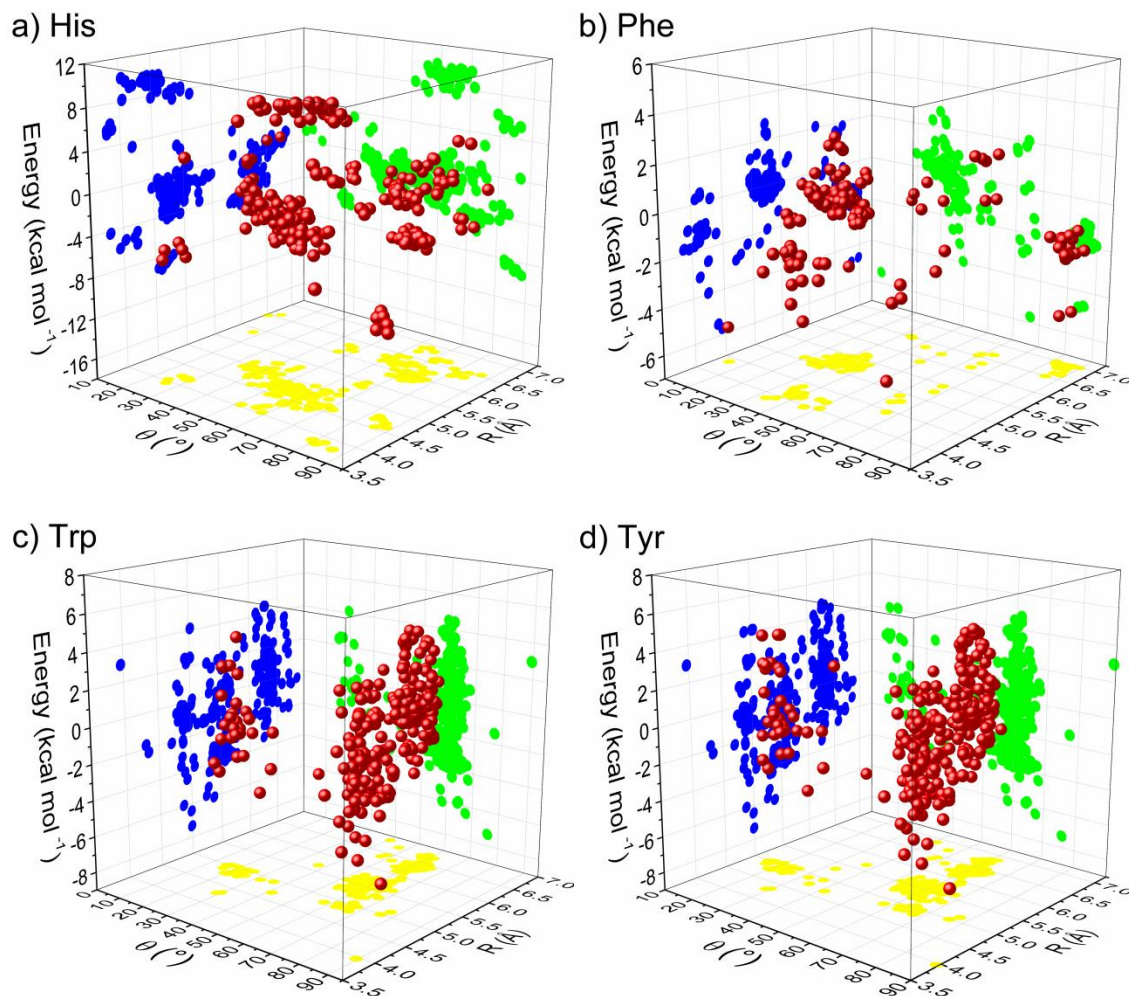

Fig. 6. 3D scatter plots from the energy analysis showing the distribution of energies depending on distance and angle for anion−π interacting pairs; (a) His, (b) Phe, (c) Trp, and (d) Tyr. A red circle denotes an energy that is an accepted anion−π interaction; yellow, green, and blue circles denote XY, XZ and YZ projections, respectively.
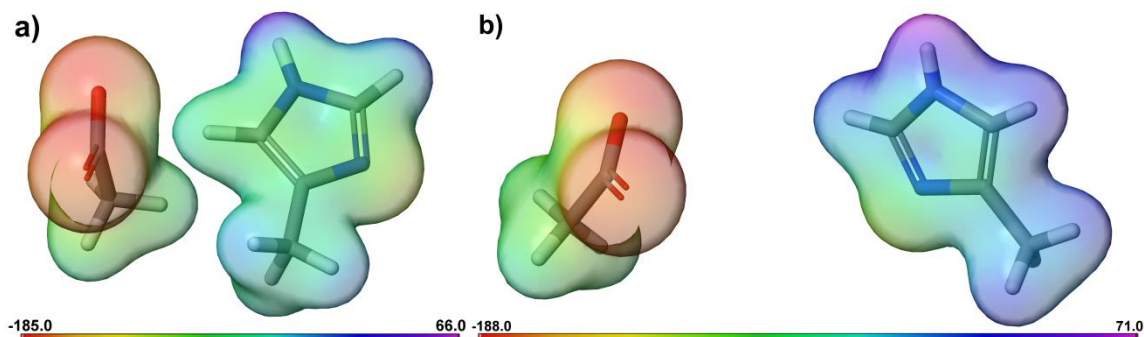
Fig. 7. ESPs mapped onto electron density isosurfaces: (a) The strongest anion−π interaction (B:Asp72:OD2—B:His88) in the Cu/Zn superoxide dismutase of *Photobacterium leiognathi* (PDB ID: 1yai), and (b) The weakest attractive predicted anion−π interaction (A:Asp165:OD1—A:His150) in the cambialistic superoxide dismutase of *Aeropyrum pernix* (PDB ID: 3ak2). Pictures were prepared by mapping values for calculated ESP of molecules onto the isodensity surface on 0.0125 electrons/bohr³. Typically, a color scale is used, with the most negative potential colored red and the most positive potential colored violet. Figure was prepared using the program Jaguar from Schrödinger Suite 2016-1 [45].
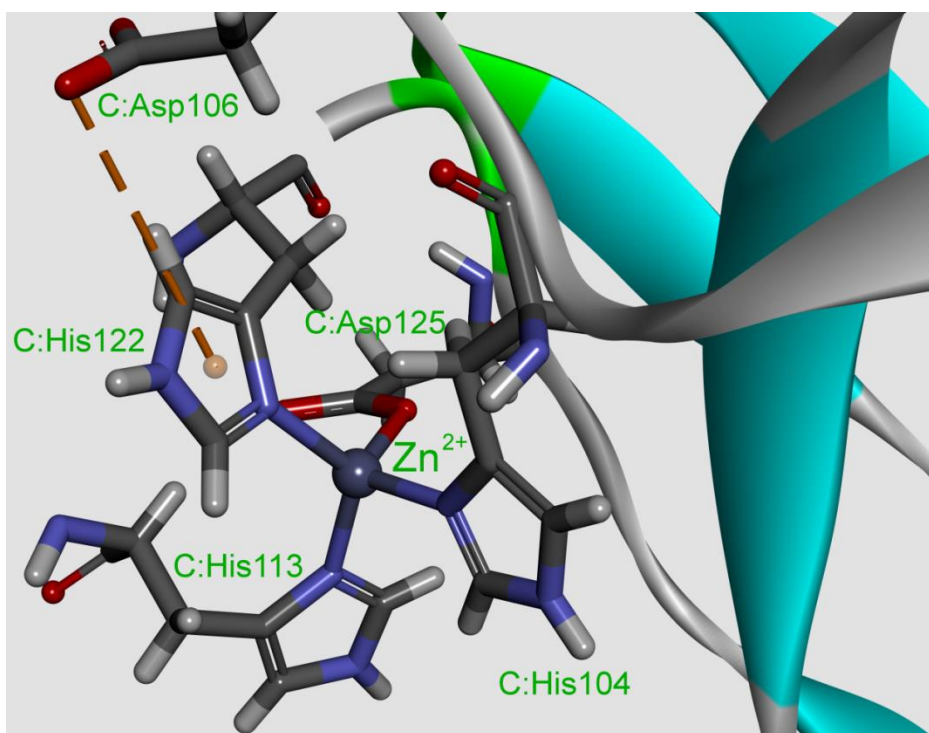

Fig. 8. Details of metal-assisted anion−π interaction of Cu/Zn superoxide dismutase from *Neisseria meningitidis* (PDB ID: 2aqn). The anion−π interaction is marked *with brown dashed line*. Letters followed by the colon on picture (e.g. C:) in front of the amino acid name on the picture are names of the protein chain. Figure was prepared using the program Discovery Studio Visualizer 4.5 [43].
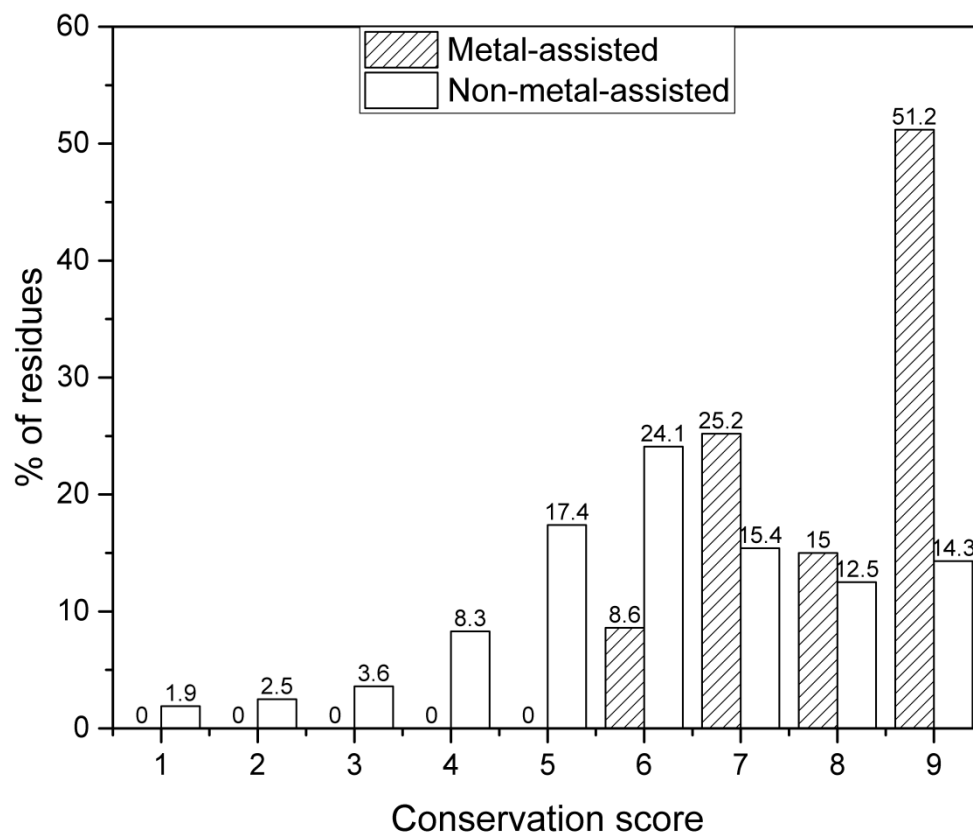
Fig. 9. Frequency of occurrence of residues at different conservation scores in superoxide dismutase active centers.
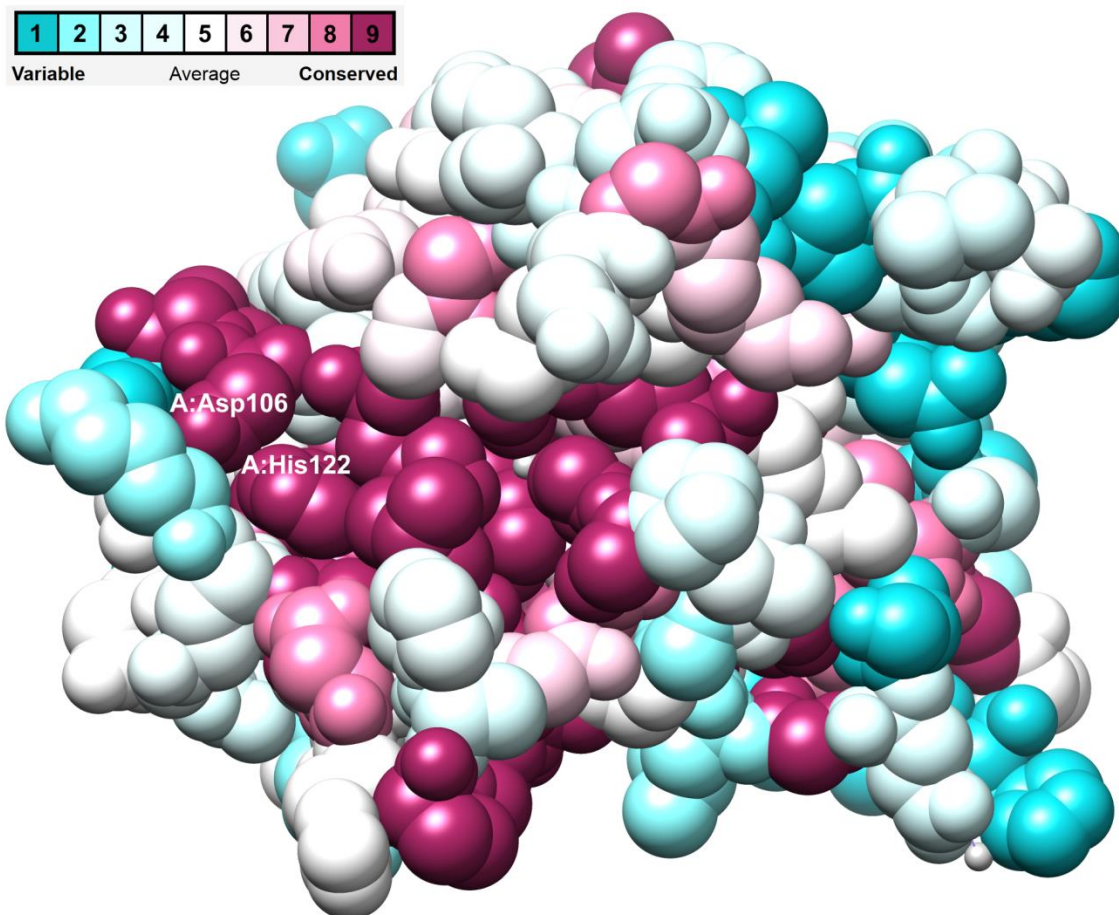
Fig. 10. Conservation pattern of Cu/Zn superoxide dismutase from *Neisseria meningitidis* (PDB ID code 2aqn; Chain A) using Chimera. Conservation score of A:Asp106 and A:His122 residues is 9. Letters followed by the colon (e.g. A:) in front of the amino acid name on the picture are names of the protein chain.

Table 1

Frequency of occurrence of anion−π interaction forming residues in active centers of superoxide dismutases.

	N^a	$\%^b$	N^c	$\%^d$	$N_{anion-\pi}{}^e$	$\%_{anion-\pi}{}^f$
Anionic amino acid						
Asp	1475	5.3	109	2.3	536	50.6
Glu	1707	6.2	267	5.7	524	49.4
Total	3182	11.5	376	8.0	1060	100
Aromatic amino acid						
His	1394	5.0	418	8.9	247	23.3
Phe	1118	4.0	256	5.5	138	13.0
Trp	668	2.4	348	7.4	429	40.5
Tyr	970	3.5	468	10.0	246	23.2

27

Total	4150	14.9	1490	31.8	1060	100

[a] The number of amino acid in the entire database

[b] Percent of amino acid in the entire database

[c] The number of amino acid in second coordination sphere of superoxide dismutase active centers

[d] Percent of amino acid in second coordination sphere of superoxide dismutase active centers

[e] Number of anion−π interactions in superoxide dismutase active centers

[f] Percent of anion−π interactions in superoxide dismutase active centers

Table 2

Involvement of stabilizing center residues in anion−π interactions of superoxide dismutase active centers.

Amino acid	$N_{anion-\pi}$[a]	SC[b]	$SC_\%$[c]
Anionic			
Asp	536	175	32.6
Glu	524	161	30.7
Total	1060	336	31.7
π residues			
His	247	104	42.1
Phe	138	54	39.1
Trp	429	133	31.0
Tyr	246	91	37.0
Total	1060	382	36.0

[a] Number of anion−π interactions in superoxide dismutase active centers

[b] Number of SC residues involved in anion−π interactions

[c] % of SC residues involved in anion−π interactions